

João Pela\*  
Imperial College London  
(Dated: October 28, 2014)

Theoretical and experimental motivations are presented for the analysis in which I am involved at the Compact Muon Solenoid experiment, the standard model Higgs on the  $\gamma\gamma$  decay channel analysis and vector boson fusion produced Higgs with invisible decay products analysis. A summary of the service work already performed is also given.

Keywords: Experimental high energy physics, trigger systems and data acquisition

## I. INTRODUCTION

The current knowledge on the field of particle physics is summarized in the standard model (SM). It is known that this model is incomplete without the inclusion of a spontaneous symmetry breaking mechanism that would explain the observation that the electroweak bosons (the W and Z particles) have mass. The easiest way to introduce such a mechanism is with the Higgs mechanism, which suggests the presence of a new particle, the Higgs boson.

After 3 years of successful operation, the experiments built on the Large Hadron Collider (LHC) at European Organization for Nuclear Research (CERN) located near Geneva, Switzerland observed of a new boson. Measurements of properties of this new particle are compatible within uncertainties with what would be expected for a SM Higgs boson.

The Compact Muon Solenoid experiment (CMS) published results where the best-fit signal strength for a SM Higgs boson mass hypothesis of  $125 \text{ GeV}$  is  $\sigma_{SM} = 0.87 \pm 0.23$ . The excess is most significantly seen in the  $\gamma\gamma$  and in the  $ZZ$  decay channel, which together are the channels with best mass resolution. A fit to these signals gives a mass of  $125.3 \pm 0.4(\text{stat.}) \pm 0.5(\text{syst.}) \text{ GeV}$ . The decay to two photons indicates that the new particle is a boson with spin different from 1[? ].

The ATLAS collaboration also presented simultaneously similar results and claim of a new neutral boson with a measured mass of  $126.0 \pm 0.4(\text{stat.}) \pm 0.4(\text{syst.}) \text{ GeV}$  [? ].

### A. Higgs phenomenology

The main processes for Standard Model Higgs production are summarized in figure 1A.

The respective cross sections for each production process can be found in figure 2 [? ]. It can be seen that the gluon fusion (GF) is the leading process by almost one order of magnitude higher than vector boson fusion (VBF) which is the second most frequent process in the currently

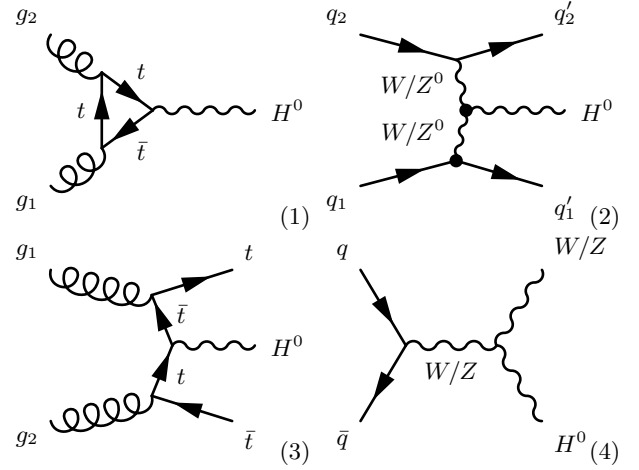


Figure 1. Main processes for standard model Higgs production ordered by highest cross section at the LHC. (1) gluon fusion, (2) vector boson fusion, (3)  $t\bar{t}$  fusion and (4) W/Z associated production.

allowed experimental mass range for a Standard Model Higgs Boson. Both  $t\bar{t}$  fusion and weak boson associated productions have cross sections more than one order of magnitude lower than VBF in the same mass range.

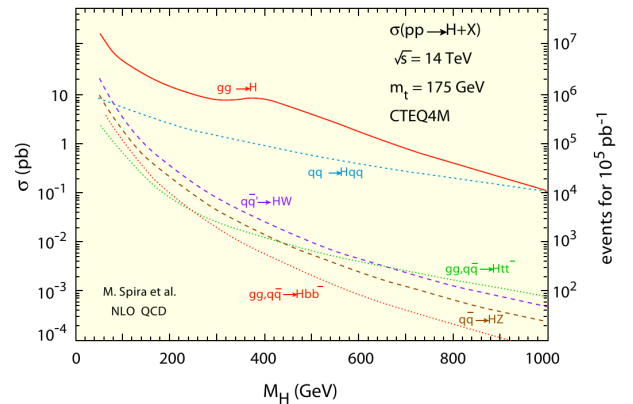


Figure 2. Theoretical prediction of standard model Higgs productions cross sections for a  $\sqrt{s} = 14 \text{ TeV}$  and assuming  $m_{top} = 175 \text{ GeV}$ .

\* joao.pela@cern.ch

The Higgs boson will then decay with different proba-

bilities to different objects depending on its mass; a plot of these probabilities can be found at figure 3 [? ].

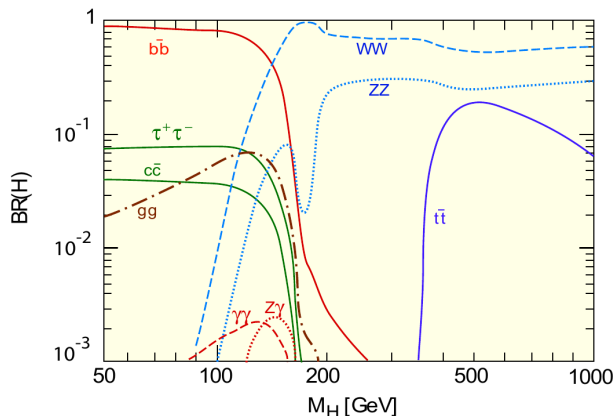


Figure 3. Theoretical prediction of standard model Higgs branching ratios as a function of its mass.

### B. Higgs to $\gamma\gamma$

The  $H \rightarrow \gamma\gamma$  channel main production mechanism is gluon fusion. This process compared with the other possible production mechanisms and decays is the one that presents the biggest potential for discovery at low masses, since its clean signature and amount of background on the signal area make this channel the most promising.

In the  $H \rightarrow \gamma\gamma$  analysis a search is made for a narrow peak in the diphoton invariant mass distribution in the range 110–150 GeV. This signal is sitting on a large irreducible background from QCD production of two photons and reducible background where one or more of the reconstructed photons originate from misidentification of jet fragments.

### C. Vector boson fusion Higgs to invisible

The first theoretical motivations for looking for VBF Higgs events is obviously to observe and measure its cross section and each of the branching ratios for its decays. We can then calculate its coupling to the weak bosons and to fermions (including the leptonic sector via  $\tau\bar{\tau}$ ). From the couplings, we may be able to differentiate between a SM Higgs or beyond the standard model (BSM) Higgs such as one of the super symmetric incarnations of this boson[? ? ]. Also for models where the Higgs would only decay invisibly, VBF is the primary discovery channel.

From the experimental point of view, we can see from figure 2 that VBF has a cross section one order of magnitude lower than GF, but we should notice from diagram 2 in figure 1A that there are two forward jets produced along with the Higgs and we can use them for tagging.

Also, we can profit from the lack of colour exchange between the interacting quarks which will result in low hadronic activity in the central rapidity region coming from the main interaction. Since the Higgs visible decay products (if any) are most likely produced in the central rapidity region, this means that they will be likely isolated from the forward jets thus allowing better reconstruction/identification efficiency which should allow easier study of the Higgs properties.

In the case of an invisible decay we can profit from the large Z to invisible decay branching ratio. On the other hand we do not have the Higgs decay products to reconstruct its mass, so we have to rely only on the missing energy and tagged jets to identify these events.

## II. EXPERIMENTAL INTRODUCTION

### A. Large Hadron Collider

The Large Hadron Collider (LHC) is at this moment the world's largest and highest-energy particle accelerator in activity. It was built in a 27 kilometer circular tunnel, at an average depth of around 100 meters, under the Franco-Swiss border near Geneva, Switzerland[? ].

The LHC is a synchrotron machine designed to accelerate and collide two opposing particle beams. Particles are injected into the machine in bunches, which can be composed of protons or lead nuclei. For protons the maximum nominal energy that can be achieved per beam is 7 TeV, which represents 14 TeV in the center of mass frame for a single proton-proton collision. For lead nuclei a maximum nominal energy of 574 TeV per nucleus (2.76 TeV per nucleon) per beam is planned. The running conditions for proton collisions during 2012 are 8 TeV center of mass energy, with an initial average number pile up collisions of the order of 28 and a delivering instant luminosity of the order of  $5 \times 10^{33} \text{ cm}^{-2} \text{ s}^{-2}$

### B. Compact Muon Solenoid

The Compact Muon Solenoid experiment (CMS) is a general purpose experiment that is an integrating part of the LHC program. It was designed to study the collisions of two intersecting proton beams in its centre [? ]. This detector was planned with the intention of studying a broad spectrum of physics processes and is made of several subsystems, each one designed to take advantage of some characteristics of the particles produced in order to measure their energy, momentum and charge. The detector has classical onion structure with several layers. Starting from the collision point outwards we have: pixel system, tracker system, electromagnetic calorimeter, hadronic calorimeter, magnet, muon systems and return yoke.

At nominal conditions, forty million collisions are produced in a single second and it would be impossible to

register all of them. As almost all collisions are uninteresting, the solution is to have an event selection already in the machine so we would only save the most interesting events. This is the role of the trigger system, which is split into two levels, where the second level benefits from the extra time from the selection at first level to access more information of what happened. Using this approach by stages we are able to reduce the number of events to a more manageable rate between of under 1500  $Hz$ .

The overall dimensions of CMS detector are a length of 21.6  $m$ , a diameter of 14,6  $m$ , and total weight of 12500  $tons$ .

### C. Trigger

During 2012, LHC is being run with 50  $ns$  bunch separations leading to a maximum bunch crossing rate of 20  $MHz$ . Data from only about  $10^3$   $events/sec$  can be written to archival media; hence, the trigger system has to achieve a rejection factor of  $\sim 2 \times 10^5$  by selecting what may be the most interesting events. The CMS trigger and data acquisition system consists of: the detector electronics, the Level-1 trigger processors (calorimeter, muon, and global), the readout network, and an online event filter system (processor farm) that executes the software for the High-Level Trigger (HLT).

### D. Level 1 trigger

The size of the LHC detectors and the underground caverns imposes a minimum transit time for signals from the front-end electronics to reach the services cavern housing the Level-1 trigger logic and return back to the detector front-end electronics. The total time allocated for the transit and for reaching a decision to keep or discard data from a particular beam crossing is 3.2  $\mu s$ . During this time, the detector data must be held in buffers while trigger data is collected from the front-end electronics and decisions are reached. This decision allows to discard a large fraction of events while retaining the small fraction of interactions of interest (nearly 1 crossing in 1000) at hardware level. Of the total latency, the time allocated to Level-1 trigger calculations is less than 1  $\mu s$ .

## III. DATA ANALYSIS

### A. Vector Boson Higgs to Invisible

#### 1. VBF Signature at CMS

The VBF SM Higgs signature main characteristic is the presence of two forward jets associated with the Higgs

(see diagram 2 in figure I A). These two forward jets have a reasonable  $p_T$  ( $\gtrsim 30$   $GeV$ ), high  $\Delta\eta$  separation between them ( $\gtrsim 3$ ) and low  $\Delta\phi$  ( $\lesssim 2.5$ ). The dijet pair also has a high invariant mass since it will be produced back-to-back to the Higgs boson. Because there is no color exchange between the incoming quarks, the hadronic activity between the jets is suppressed. On the other hand, the Higgs decay products, if any, will be located at the central rapidity area which will be easier to study because of the lower hadronic activity coming from the main interaction already described[? ].

To illustrate this separation of the SM Higgs decay products let's look at VBF Higgs decay to a pair of  $\tau$ . The distribution of the pseudo-rapidity for both forward jets and two  $\tau$  coming from SM Higgs decay of simulated events at the CMS detector can be found in figure 4.

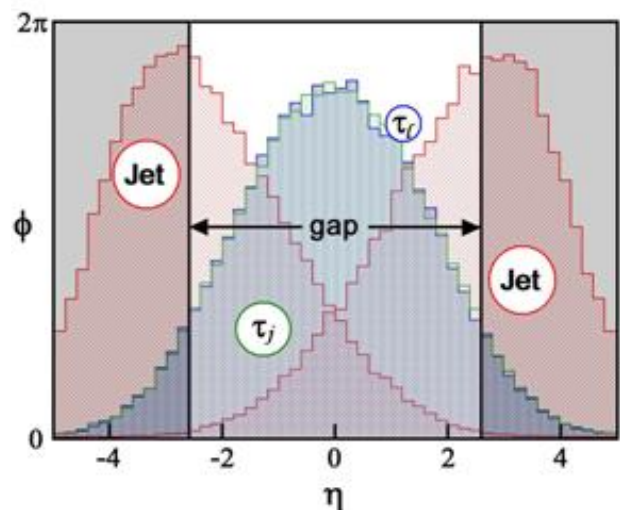


Figure 4. Simultaneous plot of the  $\eta$  coordinate of both forward jets and the  $\tau\bar{\tau}$  produced from simulated VBF Higgs decay. Super-imposed with 4 circles showing the possible positions of these 4 objects in a hypothetical event.

The CMS detector is ideal for these types of searches since it is a  $4\pi$  hermetic detector with calorimeter coverage from -5 to 5 in pseudo-rapidity. It also has very good capabilities of particle measurement and identification which can be used to identify the forward jets and Higgs decay products or in case of an invisible decay, compute the resulting missing transverse energy. An event display of a simulated Standard Model Higgs (which then decays to  $\tau\bar{\tau}$ ) produced via VBF can be found in figure 5.

#### 2. L1 Trigger Studies

The first step of any analysis is defining or selecting a trigger to collect data. This trigger should have a high signal efficiency while recording an acceptable background.

At the beginning of 2012 the possibility of recording

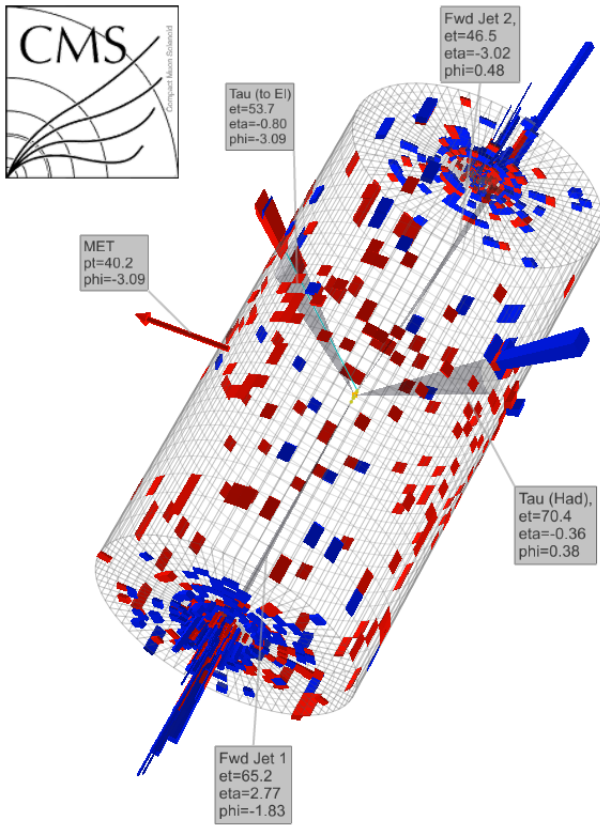


Figure 5. Event display of a simulated event where a standard model Higgs is produced via vector boson fusion which then decays to  $\tau\bar{\tau}$ , this in turn decay leptonically to an electron (left) and hadronically (right).

data without prompt reconstruction it was introduced, thus allowing to record up to 1500  $Hz$  of data where only 300  $Hz$  are promptly reconstructed. This is now known as *parked data*; this data was reconstructed after the beginning of *Long Shutdown 1* already in 2013.

A study was initiated on the possibility to use this extra bandwidth to make a set of triggers that would cover record VBF events regardless of final state.

### 3. Invisible Higgs trigger

## B. Study of variables for QCD suppression

One of the most difficult background to estimate in the VBF Higgs to invisible analysis is QCD. This is mostly due to the lack of Monte Carlo sample statistics which are very difficult to produce because of the enormous quantity of events necessary to replicate enough signal like QCD.

A possible approach is to try to reduce QCD levels where it can be considered negligible. In an attempt to use this approach we started to look for possible new variables that with a minimal signal impact would reduce

QCD event yields by several orders of magnitude.

Three new variables were studied which try to exploit the correlations of the dijet plus MET system: Scalar Tri-Object Sum, Dijet  $p_T$  fraction and Vector Tri-Object Sum.

### 1. Scalar Tri-Object Sum

This variable is defined as  $|p_T(jet1)| + |p_T(jet2)| + |MET|$  which is similar to HT but only applied to our objects of interest. This implies that the higher it is, the better the average relative object resolution. This variable can also be used to relax constraints on individual object while still enforcing a global minimum transverse energy of the combined system.

### 2. Dijet $p_T$ fraction

This variable is defined as  $p_T(dijet)/(p_T(dijet) + MET)$ . It reflects the balance of the dijet plus MET system. For signal it should peak strongly around 0.5 while this should not be the case for QCD in the case MET is faked.

### 3. Vector Tri-Object Sum

This variable is defined as  $|VectorSum(p_T(jet1) + p_T(jet2) + MET)|$ . It also reflects the balance of the dijet plus MET system. In this case, value of the variable for signal should concentrate around zero with the spread defined by the jet and MET resolution. The possibility of using jet and MET resolution as an input to this variable is being studied.

### 4. Combining variable

Based on the method of some CMS SUSY analysis that use an HT cut in conjunction with the  $\alpha_T$  variables, a study was performed to evaluate the possibility of combining the scalar tri-object sum with each of dijet plus MET variables. Two dimensional plots for the signal monte carlo after the MET cut on the official VBF to invisible analysis can be seen in fig 6 for dijet  $p_T$  fraction versus scalar tri-Object sum and fig 7 for vector tri-object sum versus scalar tri-object sum.

Preliminary studies show that by defining a 2D cut on these pairs of variables could yield a reduction of a factor of 2.5 on QCD, Z+Jet and W+Jets with a signal loss of less than 30%.

These studies may prove especially valuable for use in parked data, since by applying constraints on this type of system variables we may be able to relax cut on jet  $p_T$  and MET and therefore increase signal yield making use of the lower trigger thresholds for these individual objects,

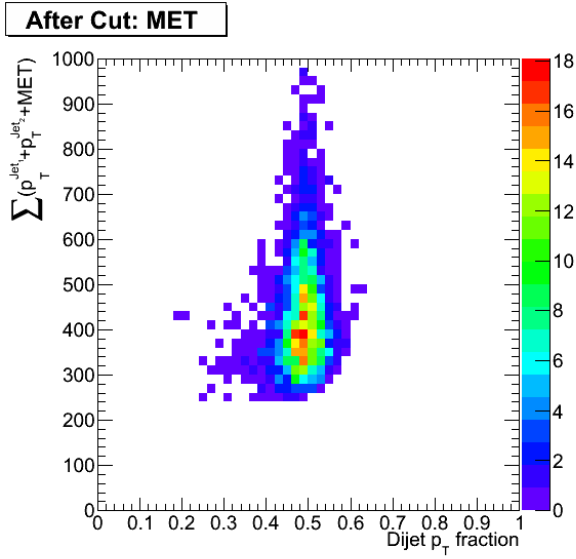


Figure 6. Plot of dijet  $p_T$  fraction versus scalar tri-object sum for signal monte carlos  $m_H = 120 \text{ GeV}$  after the MET cut of the official VBF to invisible analysis.

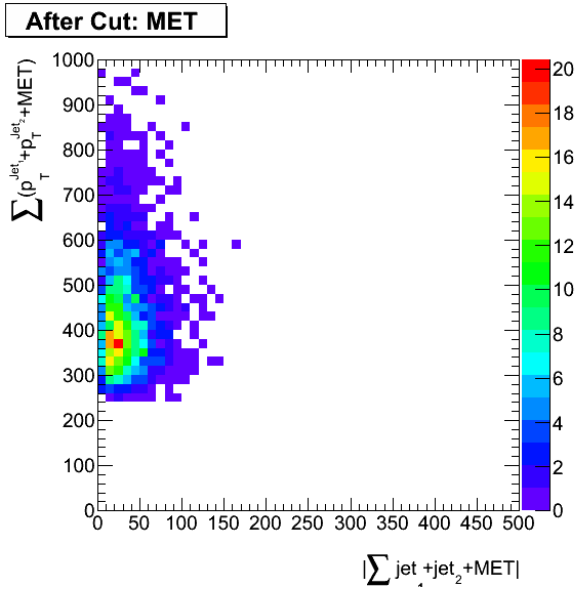


Figure 7. Plot of vector tri-object sum versus scalar tri-object sum for signal monte carlos  $m_H = 120 \text{ GeV}$  after the MET cut of the official VBF to invisible analysis.

while keeping or even improving signal to background ratio.

#### IV. RUN II PREPARATION

---

David Colling (Supervisor)

---